



OPEN Optimization of sporulation of *Trametes sanguinea* ZHSJ and untargeted metabolomics of spores, mycelium and fruiting body

Yunmei Li^{1,2,7}, Yuting Su^{1,2,7}, Peng Yang⁶, Chune Peng^{2✉}, Xiaoyi Cheng³, Xiao Zhang³, Lizeng Peng^{2,3,4,5✉}, Rathna Silviya Lodi^{2,4✉} & Zhixin Wang^{1✉}

Trametes sanguinea belongs to the polyporaceae family and it is a white rot medicinal fungus. In the present study, pure mycelium of *Trametes sanguinea* ZHSJ (*T. sanguinea* ZHSJ) was obtained from the fruiting body of wild basidiomycetes by tissue separation method, and its growth conditions were optimized in vitro. The results exhibited the optimal growth of *T. sanguinea* ZHSJ at pH 5, temperature 30 °C with the carbon source maltose 20 g/L and nitrogen source yeast extract 4 g/L. LC-MS based untargeted metabolomic studies revealed there are 6715 metabolites in both positive and negative ion mode detection of spores (SP), mycelium (MY) and fruiting body (MU). However, principal component analysis (PCA) represented PC1 67.10% and PC2 24.60% metabolite variance among SP, MY and MU. Further, metabolite cluster and Variable projection importance (VIP) analysis has represented differential upregulated and down regulated metabolites with p value < 0.05 and VIP ≥ 1 significance. Moreover, KEGG pathway enrichment analysis represented SP vs. MY and SP vs. MY major metabolites 23 and 31 involved in biosynthesis of co-factors and MY vs. MU major metabolites involved in diterpenoid biosynthesis. Hence, current study reveals that the morphological stages of *T. sanguinea* ZHSJ possess several variations in their metabolites and this is the first study to reveal the optimization of *T. sanguinea* spores and their metabolites comparison with mycelium and fruiting body through LC-MS based untargeted metabolomics. Further research on the biological activity of these differential metabolites of *T. sanguinea* spores would way a path in identification of novel medicinally important compounds.

Keywords *Trametes sanguinea*, Growth optimization, Viable spores, LC-MS, Untargeted metabolomics

Trametes sanguinea belongs to the Polyporaceae family¹, grows on the fallen trees, stumps, and rotten wood of broad-leaved trees, occasionally on conifers and its distribution is strongly associated with sun-exposed habitats and forest edges. The fruiting body of *T. sanguinea* is annual and woody, often appearing in summer and autumn, and is closely attached to the substrate which makes it difficult to harvest². The fruiting bodies of *T. sanguinea* are rich in nutrients, hence, in some East Asian countries such as China, they are often used in soups and stews, not only to enhance the flavor of the food but also used as mineral and protein supplements³. As a white-rot fungi, *T. sanguinea* degrades lignocellulose by secreting laccase extracellularly, lignin initially gives wood its brown color, but it turns white after being infected by white-rot fungus⁴⁻⁶. Due to its degradation potential, it is also commonly used in wastewater treatment, food processing and other fields⁶⁻⁸.

¹College of Food and Biology, Hebei University of Science and Technology, Shijiazhuang 050018, China. ²Key Laboratory of Agro-Products Processing Technology of Shandong Province, Key Laboratory of Novel Food Resources Processing Ministry of Agriculture, Institute of Food & Nutrition Science and Technology, Shandong Academy of Agricultural Sciences, Jinan 250100, China. ³School of Pharmacy, Shandong University of Traditional Chinese Medicine, Jinan 250355, China. ⁴Jinan Asia Pharmaceutical Technology Co., Ltd., Jinan 250100, China. ⁵State Key Laboratory of Natural Product Chemistry, Lanzhou University, Lanzhou 730000, China. ⁶State Key Laboratory of Nutrient Use and Management, Key Laboratory of Wastes Matrix Utilization, Ministry of Agriculture and Rural Affairs, Institute of Agricultural Resources and Environment, Shandong Academy of Agricultural Sciences, Jinan, China. ⁷Yunmei Li and Yuting Su contributed equally to this work. ✉email: pengchune@saas.ac.cn; penglizeng@sdu.edu.cn; 15954128918@163.com; silviya.lodi@gmail.com; zhixwang0311@163.com

Furthermore, *T. sanguinea* is also a medicinal fungus, several studies represented that the various active substances such as terpenoids, polysaccharides and sterols^{9,10} exhibit significant pharmacological activities, such as antitumor, antibacterial, anti-inflammatory and immune-enhancing effects^{3,11,12}. In recent decades, polysaccharides from medicinal fungi have attracted extensive interest from researchers worldwide due to their high anti-tumor activity and low side effects^{13–15}. Some studies demonstrated that polysaccharides extracted from fungi can act as natural immune modulators¹³.

Recent studies on medicinal macro fungi have predominantly focused on secondary metabolites derived from mycelia and fruiting bodies, particularly polysaccharides, triterpenoids, and phenolic compounds with demonstrated pharmaceutical potentials^{16,17}. However, growing evidence suggests that fungal spores may represent a unique and underexplored repository of bioactive substances. During sporulation, fungi undergo specialized metabolic reprogramming to synthesize stress-resistant compounds that are typically absent or present in minimal quantities within vegetative tissues^{18–20}. Despite these advances, the biochemical potential of *T. sanguinea* spores remains largely uncharted. Current research on this species has prioritized laccase production from fruiting bodies and antioxidant profiling of mycelial extracts^{21,22} leaving its spore-derived components systematically uncharacterized. The spores of *T. sanguinea* formed by the fragmentation of hyphae, so the number of spores inseparably related to the length and quality of the hyphal body. The purpose of optimizing the growth conditions of hyphal bodies is to obtain more healthy hyphae, which can solve the problem of a small number of spores, which is a prerequisite for the subsequent induction and collection of spores. The striking orange-red pigmentation observed in *T. sanguinea* fruiting body is a phenotypic trait potentially linked to naphthoquinone (a class of redox-active aromatic compounds) biosynthesis, which provides compelling rationale for investigating their antioxidant metabolite profiles²³.

In recent years, with the increasing research on the medicinal value of *T. sanguinea*, it has shown that the chemical components of the fruiting body and mycelium of *T. sanguinea* are similar^{3,10,12}. The spores, mycelium and fruiting body are different morphological stages in the life cycle of fungi, and they have obvious differences in morphology, structure and function¹⁷. However, the metabolites of *T. sanguinea* spores were yet to be known and there is a lack of comprehensive analysis to differentiate the key metabolites in the spores, mycelium and fruiting body of *T. sanguinea*. Therefore, to better develop and utilize the resources of *T. sanguinea*, it is necessary to systematically analyze the chemical components of different morphological stages of *T. sanguinea*.

At present, there are few studies on the active ingredients of *T. sanguinea*, and most of them adopt a single detection technology, such as gas chromatography-mass spectrometry (GC-MS), high performance liquid chromatography (LC-MS) and other techniques, which can only detect a few components. Untargeted metabolomics is a method that can systematically and comprehensively analyze the endogenous metabolites in biological organisms²⁴. It can analyze the types, quantities and changes of small molecular metabolites in biological systems. Traditional analysis technology can only detect a certain type or several types of components. Metabolomics comprehensively and systematically carry out metabolite analysis and combine multivariate statistical analysis efficiently and screen characteristic differential metabolites, which have been widely used in the field of microorganisms.

Therefore, in current study, we conducted a comprehensive investigation for the first time to collect the spores by several optimization conditions and analyzed their viability, morphology and germination potentiality of *T. sanguinea* ZHSJ and further we have analyzed for the presence of differential metabolites in spores by comparing with the other morphological stages of fungi that is mycelium and fruiting body through LC-MS based untargeted metabolomics analysis, (Fig. 1), thereby transcending the current narrow understanding of this fungus spores.

Materials and methods

Isolation and identification of fungus

Sample collection

Red-colored fruiting bodies morphologically consistent with *T. sanguinea* were collected by Lizeng Peng from the Mengyin Yun Meng scenic area, Linyi city, Shandong Province, China. Samples were aseptically transferred to sterile sampling bags, promptly transported to the laboratory, and stored at 4 °C for further analysis.

Isolation of fungi

The pure mycelium of *T. sanguinea* strain was obtained by tissue culture techniques. Under aseptic conditions in a laminar flow cabinet, fruiting bodies were surface sterilized by cleaning with sterile water, followed by disinfection with 75% (v/v) ethanol 3 times to ensure the surface impurities were completely removed. Then, it was washed with sterile water 5 times, and the sterile water on the surface was completely removed by sterile absorbent paper. Approximately, 100 µL of the final rinse water was inoculated on Potato Dextrose Agar medium (PDA) (Haibo Biotechnology Co., Ltd., Qingdao, China) to examine surface sterilization. Further, *T. sanguinea* samples were cut into 0.5 cm × 0.5 cm pieces with a sterile scalpel and placed on PDA, followed by incubation at 28 °C for 4–7 days for fungal growth. After 7 days, white velvety mycelium was observed around the fruiting body pieces, then mycelium was inoculated onto a new PDA plate and incubated at 28 °C for 7–14 days to obtain the pure *T. sanguinea* mycelium and named as *T. sanguinea* ZHSJ. *T. sanguinea* ZHSJ has been stored at China General Microbiological Culture Collection Center with deposit number 40866. This procedure allowed pure cultures to be obtained, which were preserved for further study.

Morphological identification

The macroscopic characterization of *T. sanguinea* ZHSJ, such as color, shape, and growth location of the wild fruiting bodies were first observed and their length, width, and height were measured and recorded. The mycelium was cultured in the dark at 28 °C on PDA for 14 days, during which the morphological and color

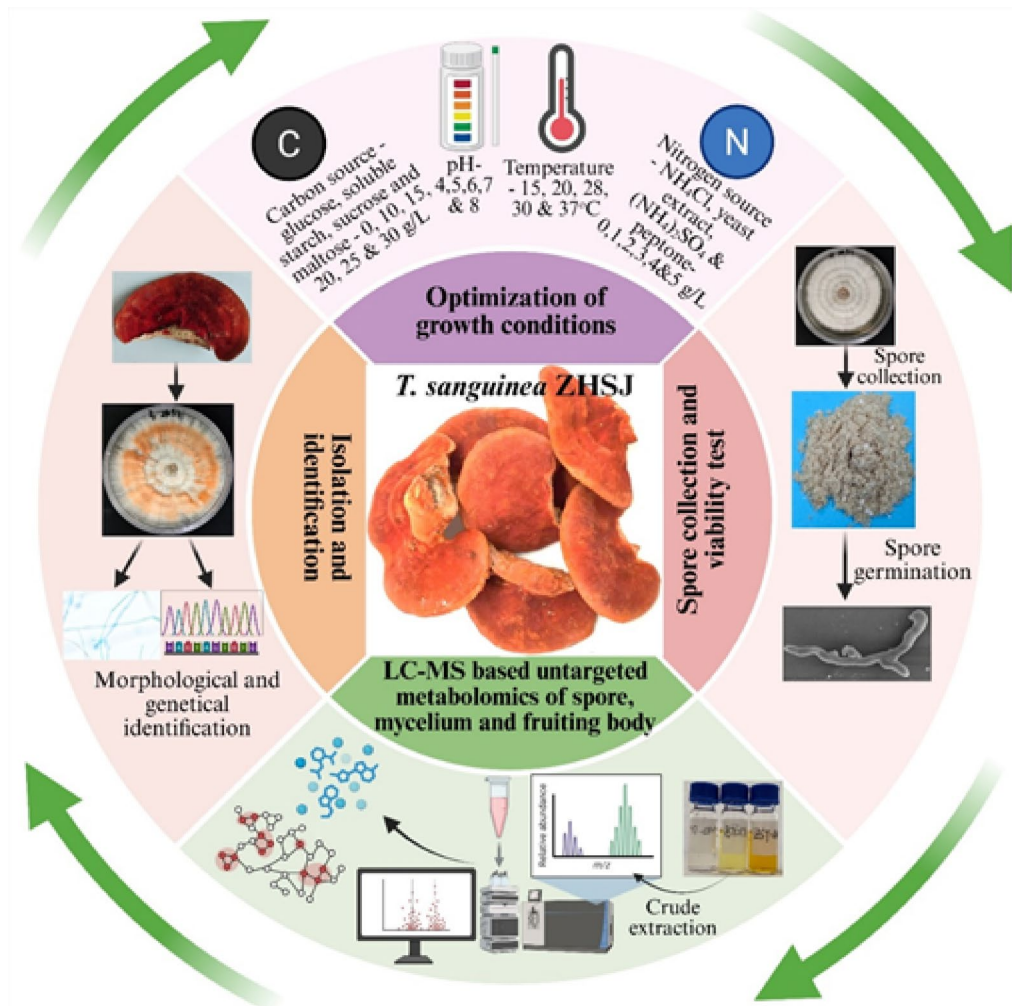


Fig. 1. The overall outline of the *Trametes sanguinea* ZHSJ spores.

changes of the mycelium were observed and recorded. The mycelium was subjected to Lactophenol Cotton Blue staining to analyze the structure of the mycelium and spores using the 40× and 100× magnifying lenses of an upright microscope. Images of *T. sanguinea* ZHSJ were obtained by using scanning electron microscopy (SEM) (VEGA3, Tescan L TD., Czech Republic) to observe the morphology of hyphae and spores. The magnifications of the image were 2000× and 10,000×.

Genetical identification

Fungal DNA was extracted by using a Biospin Fungi Genomic DNA Extraction Kit (Hangzhou Bioer Technology Co., Ltd., China) following the manufacturer's instructions. The 18S rRNA internal transcribed spacer regions (ITS) of the *T. sanguinea* ZHSJ was amplified by PCR using the universal primers 18SF (5'AACTTAAAGGAATT GACGGAAG 3') and 18SR (5'TCCGCAGGTTACCTACGGA 3') along with the ReadyMix™ Taq PCR mix with MgCl₂ (Sigma Aldrich, USA). PCR reaction conditions: 98 °C pre-denaturation for 5 min, 98 °C denaturation for 15 s, annealing at 60–68 °C for 30 s, extension at 72 °C for 1 min, and these steps were repeated thirty times. Later 72 °C extensions for 10 min and stabilization at 4 °C for 10 min. Then the PCR products were recovered and by agarose gel electrophoresis with an AxyPrep DNA gel extraction kit (Axygen, USA) for sequencing. These sequences were aligned with the NCBI database, and the relevant sequences from GenBank were downloaded. The phylogenetic tree was constructed using the Neighbor-Joining method in MEGA11 software.

Optimization of *T. sanguinea* ZHSJ growth conditions

pH

The optimum pH that favors the growth of *T. sanguinea* ZHSJ was analyzed by adjusting the pH of Potato Dextrose Water (PDW) (Haibo Biotechnology Co., Ltd., Qingdao, China) (150 mL) and PDA plates with pH 4, 5, 6, 7 and 8 by using 1 M NaOH and 1 M HCl before autoclave. A 5 mm diameter mycelial disc from 7 days old *T. sanguinea* ZHSJ plate was cut and added to the PDW and placed at the center of the PDA plates. PDW cultures were incubated in shaking incubator 120 r/min, 28 °C, PDA plates were incubated at 28 °C. The mycelia grown in

PDW for seven and fourteen days were centrifuged at 8000 g for 10 min and freeze-dried, and their weights were recorded. The mycelial diameter of the *T. sanguinea* ZHSJ grown on PDA was measured in 7 days.

Temperature

The optimum temperature for the growth of *T. sanguinea* ZHSJ was evaluated from the temperature ranging 15, 20, 28, 30, and 37 °C. The growth of *T. sanguinea* ZHSJ was analyzed by its growth on PDA and in PDW incubated at different temperatures for about 7–14 days. The diameter of the mycelium growth on PDA and the dry weight of the mycelium growth in PDW represents the optimum temperature for the growth of *T. sanguinea* ZHSJ.

Carbon source

The carbon source suitable for optimum growth of *T. sanguinea* ZHSJ has been analyzed by using several sugars in PDA and PDW, such as glucose, soluble starch, sucrose and maltose with different concentrations 0, 10, 15, 20, 25, 30 g/L. Optimum growth with reference to carbon source was performed in two ways one is by solid culturing and another is liquid culturing. The growth diameter of the mycelium was measured on solid medium and the dry weight was measured as the optimum growth index in the liquid medium. The growth of these carbon sources was compared with the PDA and PDW growth of *T. sanguinea* ZHSJ.

Nitrogen source

The nitrogen source for the optimum growth of *T. sanguinea* ZHSJ was analyzed by infusing PDA and PDW with several nitrogen sources such as NH₄Cl, yeast extract, (NH₄)₂SO₄ and peptone with several concentrations such as 0, 1, 2, 3, 4 and 5 g/L. The infused PDA and PDW were inoculated with a disc of freshly grown *T. sanguinea* ZHSJ and incubated at 28 °C for 7–14 days in shaking or normal incubator. The optimum nitrogen source was analyzed by the diameter of *T. sanguinea* ZHSJ grown on PDA and the dry weight of the mycelium grown in PDW.

Spore collection and viability analysis

Spore collection

The optimum growth conditions were stabilized and selected for the growth of *T. sanguinea* ZHSJ and spore collection was performed by using these optimum growth conditions to obtain the viable spores. Under suitable growth conditions, *T. sanguinea* ZHSJ preferentially carries out saprophytic growth, that is, mycelium expansion. When mycelium grows to fill the entire plate, *T. sanguinea* ZHSJ produces many spores due to nutrient exhaustion. Harvesting spores with a brush or scraper might damage these structures and alter the age composition of the spores, hence, the collection of conidia from *T. sanguinea* ZHSJ was performed according to the method of Jae Su Kim et al. (Kim et al., 2010) by using polysiloxane polyether copolymer (siloxane) (Aladdin, USA). Conidia on PDA plates were serially collected by washing the PDA plates with the low (0.01%) and high (0.08%) concentration of siloxane solution. First, 3 mL of a 0.01% (v/v) siloxane solution was added to the centrifuge tube containing three agar discs (10 mm diameter). Later, glass beads were added to the centrifuge tube, that facilitates in displacing the conidium. The tube was vortexed for 30 s to release maximum conidium from the three discs into the solution. The spore suspension was transferred to the new test tube and 3 mL of 0.08% (v/v) silicone solution was added to the centrifuge tube which contained the agar discs at the beginning. Then, the spore suspension was aspirated into a new test tube and 3 mL of 0.16% (v/v) siloxane solution was added to the centrifuge tube which contains agar discs at the beginning. Then, the spore suspension was filtered with 3 layers of 75 µm sterile gauze to remove the agar debris or mycelium. The collected spores were counted by using cytometer (400×) and the percentage of spores in each siloxane solution was calculated as $(N_{0.01\%} \text{ or } N_{0.08\%}) / (N_{0.01\%} + N_{0.08\%}) \times 100\%$, where $N_{0.01\%}$ and $N_{0.08\%}$ refer to the number of spores collected in 0.01% and 0.08% siloxane solutions. This experiment was repeated three times on the same day using different batches of cultures. The collected conidium suspension was freeze-dried, and the spore powder was stored in a 4 °C refrigerator for subsequent experiments.

Spore viability test

The viability of spores was tested by suspending the lyophilized spores 0.1 mg in 1 mL of sterile distilled water and inoculate into 10 mL of PDW and incubated for 0, 6, 12 and 24 h. Results were calculated by testing the OD values at 540 nm as mean value calculated by standard deviation. Subsequently, 100 µL of the spore suspension after 24 h was inoculated onto the PDA plate and incubated at 28 °C for 7–14 days.

Spore germination test

The lyophilized spore powder was suspended in sterile distilled water with concentration 1×10^7 CFU/mL and inoculated into 5 mL PDW and incubated in shaking incubator at 28 °C and 180 rpm. The germination of the spore was observed in specific time intervals such as 0, 6, 12, and 24 h by using SEM.

Extraction method

The samples spores (SP) that were produced by above optimized conditions were collected by above said method that is by growing mycelium on plate and then separation of spores from the mycelium by above said method, mycelium (MY) grown in PDW was separated by centrifuging the liquid culture at 8000 g for 10 min and fruiting body (MU) of *T. sanguinea* ZHSJ and each weighing 20 ± 5 mg were transferred into 2 ml centrifuge tube and 6 mm diameter grinding beads were added and 400 µL of extraction solution (methanol: water = 4:1 (v: v) containing four internal standards 0.02 mg/ml L-2- chlorophenyl alanine, etc.) were added and frozen in six replicates each²⁵. Then, the frozen tissues were grinded for 6 min at –10 °C, 50 Hz and followed by ultrasonic extraction (SCIEN TZ-IID, Xinzhi Biotechnology Co., Ltd., Ningbo, China) for 30 min at 5 °C, 40 kHz. Then,

sample was allowed to stand for 30 min – 20 °C and centrifuged at 13000x g, 4 °C for 15 min. Then, supernatant was transferred to a vial and stored for further analysis. Then 20 µL of each sample was transferred separately and mixed where this serves as quality control sample (QC).

UHPLC MS/MS analysis for untargeted metabolomics

T. sanguinea ZHSJ SP, MY and MU extracts of were analyzed by LC-MS through using UHPLC Exploris 480 system. The chromatographic column ACQUITY UPLC HSST3 (100 mm × 2.1 mm i.d, 1.8 µm; water, Milford, USA) was used. Here, mobile phase A is 95% water and 5% acetonitrile (containing 0.1% formic acid), mobile phase B is 47.5% acetonitrile, 47.5% isopropanol and 5% water (containing 0.1% formic acid) were used for chromatographic conditions. Whereas, for mass spectrometry conditions, samples were ionized by electrospray ionization and mass spectral signals (ESI-MS) were collected in both positive and negative ion scanning modes with the dynamic exclusion and mass scan range from 100 to 1500 m/z at a scan rate of 40 Hz. Mass spectrophotometry parameters were represented in the following table (Table 1).

Data acquisition and processing

The raw data was imported into the metabolomics processing software Progenesis QI v3.0 (Waters Corporation, Milford, USA) for baseline filtering, peak detection, integration, retention time correction, and peak alignment, ultimately resulting in a data matrix containing information such as retention time, mass-to-charge ratio, and peak intensity. Subsequently, this software was used for feature peak library identification, matching MS and MS/MS spectral information with metabolite databases. The MS mass error was set to less than 10 ppm, and metabolites were identified based on the scoring of secondary mass spectrum matching. The main databases used were mainstream public databases such as <http://www.hmdb.ca/> and <https://metlin.scripps.edu/>, as well as a self-built database. The raw data obtained by LC-MS analysis were pre-processed and corrected by further by several metabolomics softwares. Principal component analysis (PCA) and differential metabolite analysis-multivariate analysis by ropls (R packages) v1.6.2. ropls source: R/ropls-package. R. R Cluster analysis and Kyoto Encyclopedia of Genes and Genomes (KEGG) by scipy (python) v1.0.0.0. SciPy 1.0.0 Release Notes — SciPy v1.0.0 Reference Guide. Variable projection importance (VIP) analysis by ropls (R) and scipy (python) v1.6.2 and v1.0.0 and Venn pictures by Venn diagram (R packages) CRAN: Package VennDiagram.

Result

Morphological and genetical identification of *T. sanguinea* ZHSJ

The fruiting body of the *T. sanguinea* ZHSJ polypore grows in overlapping layers or as a single layer. The cap is fan-shaped, with a smooth surface and concentric rings, the edge is light orange, and wavy, the flesh is pale pink and corky (Fig. 2A). The mycelium of *T. sanguinea* ZHSJ was initially white, velvety, and had a ring-like pattern on PDA, after 5 days of incubation, some part of the mycelium turns orange. The morphology of mycelium represents obvious clamp connection structure, which is a typical feature of Basidiomycota fungi. The spores were observed elliptical under the oil lens and cylindrical under the SEM, with a relatively smooth surface, the size was about 1 × 4 µm, and the color is white (Fig. 2A–D). By using the BLAST program to align Genbank sequences, *T. sanguinea* ZHSJ and *T. sanguinea* SDBR-CMUNK0189 (GenBank accession number: MW267631.1) and *T. sanguinea* WRF-5 (GenBank accession number: MT340981.1) were clustered into one phylogenetic branch, with a bootstrap value of 69 (Fig. 2E). Based on the combination of morphological identification and molecular identification, the strain was identified as *Trametes sanguinea*.

Optimization results of *T. sanguinea* ZHSJ spore growth conditions

Optimum pH

The optimum pH was analyzed by culturing *T. sanguinea* ZHSJ spores in different pH such as 4, 5, 6, 7 and 8. However, *T. sanguinea* ZHSJ showed optimal growth at pH 5, the colony diameter was 7.4 cm which is comparatively higher than other pH (Fig. 3A). Moreover, *T. sanguinea* ZHSJ grown in liquid medium, its mycelium dry weight at pH 5 represented 5.15 g/l, which is comparatively higher than the other pH (Fig. 3C). Hence, pH 5 was represented as the optimum pH for *T. sanguinea* ZHSJ.

S: No	Description	Parameter
1.	Scan type (m/z)	70–1050
2.	Sheath gas flow rate (arb)	50
3.	Aux gas flow rate (arb)	15
4.	Heater temp (°C)	400
5.	Capillary temp (°C)	350
6.	Spray voltage (+) (v)	3400
7.	Spray voltage (-) (v)	-2800
8.	S - Lens RF Level	50
9.	Normalized collision energy (%)	20, 40, 60
10.	Resolution (Full MS)	60,000
11.	Resolution (MS ²)	7500

Table 1. Mass spectrophotometry parameters.

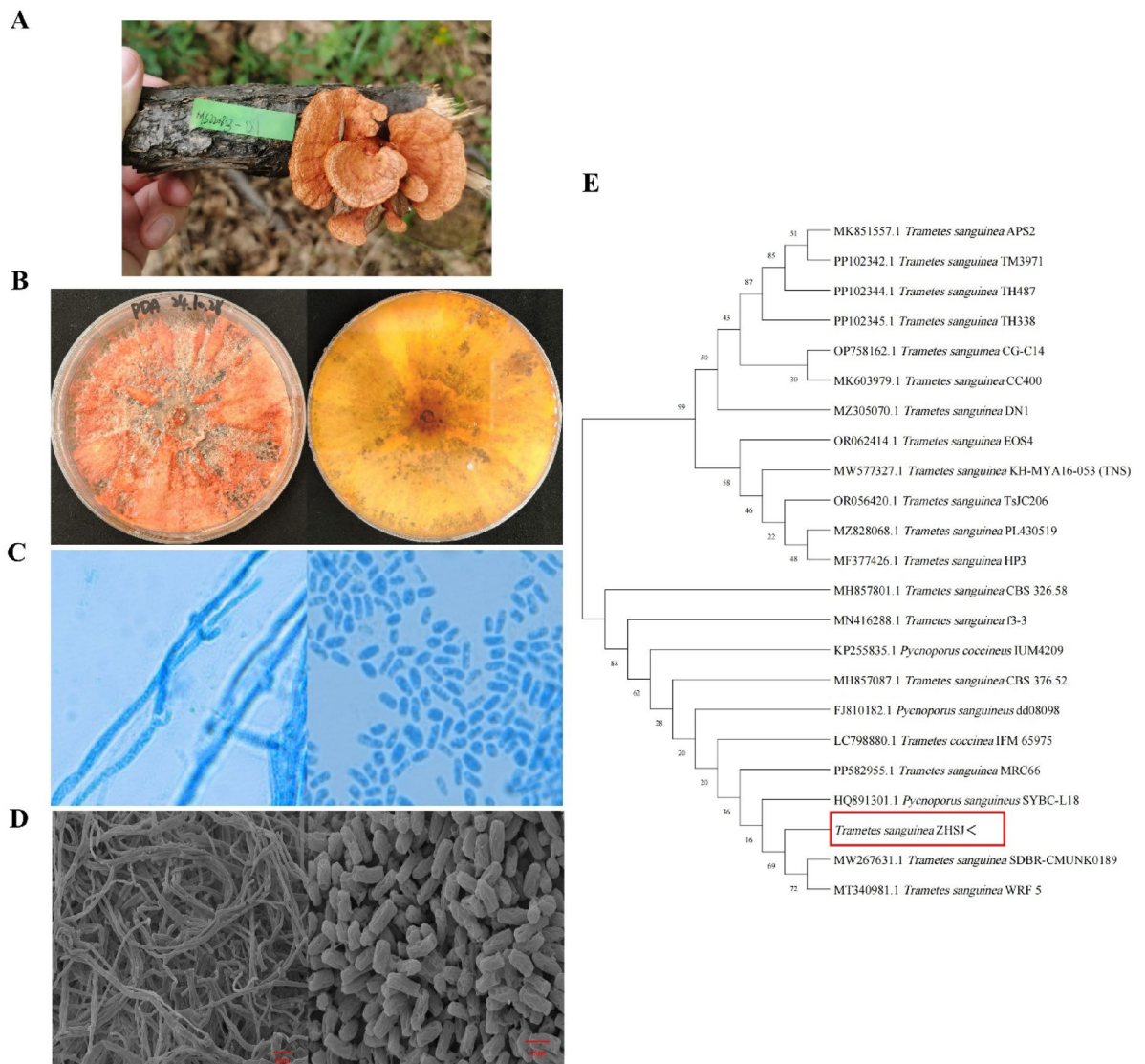


Fig. 2. Morphological and genetical identification of *T. sanguinea* ZHSJ. (A) Fruiting body of *T. sanguinea* ZHSJ. (B) The mycelium of *T. sanguinea* ZHSJ growing on PDA upward and backward images. (C) Microscopic observation of hyphae and spore structure at 40 × and 100 ×. (D) SEM observation of hyphae and spore structure at 2000 × and 10,000 ×. (E) The phylogenetic tree of *T. sanguinea* ZHSJ.

Optimum temperature

The optimum temperature of *T. sanguinea* ZHSJ spores was analyzed by culturing the fungi in several temperatures such as 15 °C, 20 °C, 28 °C, 30 °C and 37 °C in both PDA and PDW and adjusted pH of the culture medium to 5 at the same time. The optimum growth of the mycelium has been observed at the temperature 30 °C with the diameter of the mycelium was 8.3 cm and there was a dense orange colored mycelium (Fig. 3B). Simultaneously, the mycelium grown in liquid culture at temperature 30 °C represented more dry weight 6.73 g/l compared to other temperatures, hence 30 °C was represented as the optimum temperature for the growth of *T. sanguinea* ZHSJ (Fig. 3C).

Effect of carbon sources

Optimization of carbon sources was carried out by adding different carbohydrates to PDA and altering the concentration. However, among the four carbon sources, glucose, soluble starch, sucrose and maltose evaluated in this experiment, the mycelium of *T. sanguinea* ZHSJ showed optimum growth with maltose, its diameter was measured 8.27 cm which is highest when compared to others (Fig. 3D). Additionally, the liquid culturing of *T. sanguinea* ZHSJ with maltose concentration 20 g/L evinced highest dry weight 12.08 g/l, when compared to others of the Hence, maltose is referred to as the optimal carbon source for optimum growth of *T. sanguinea* ZHSJ. Other substrates, such as soluble starch, sucrose, and glucose, are ranked in descending order (Fig. 3F).

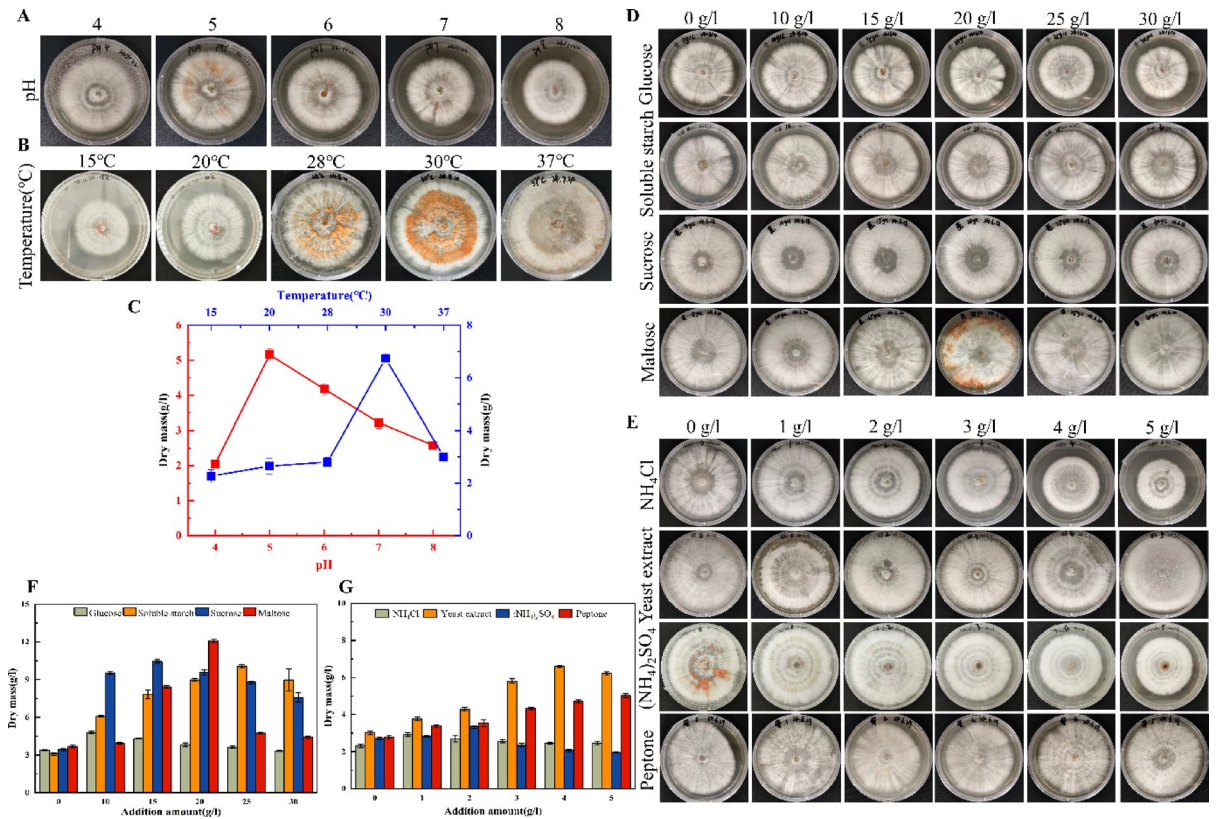


Fig. 3. Optimum the conditions of *T. sanguinea* ZHSJ spores. **(A)** Growth of *T. sanguinea* ZHSJ under different pH conditions on PDA. **(B)** Growth of *T. sanguinea* ZHSJ under different temperature conditions on PDA. **(C)** The dry weight of the mycelium of *T. sanguinea* ZHSJ cultured for 14 days under different pH and temperature conditions. **(D)** Growth of *T. sanguinea* ZHSJ under different carbon source conditions on PDA. **(E)** Growth of *T. sanguinea* ZHSJ under different nitrogen source conditions on PDA. **(F)** The dry weight of the mycelium of *T. sanguinea* ZHSJ cultured for 14 days under different carbon source conditions. **(G)** The dry weight of the mycelium of *T. sanguinea* ZHSJ cultured for 14 days under different nitrogen source conditions.

Effect of nitrogen sources

The optimum nitrogen source was identified for the growth of *T. sanguinea* ZHSJ by adding several nitrogen sources such as NH_4Cl , yeast extract, $(\text{NH}_4)_2\text{SO}_4$ and peptone with varied concentrations such as 0, 1, 2, 3, 4 and 5 g/L to the basal medium. However, *T. sanguinea* ZHSJ possessed optimum growth with 4 g/L of yeast extract. On PDA *T. sanguinea* ZHSJ evidenced 8.3 cm diameter which is the among all the nitrogen sources and their concentrations (Fig. 3E). Moreover, the dry weight of the mycelium was 6.6 g/l with 4 g/L of yeast extract which is highest among all the nitrogen sources and their concentrations. Hence, yeast extract was represented as the optimum nitrogen source for the growth of *T. sanguinea* ZHSJ (Fig. 3G).

Spore viability and germination

To analyze the viability of the spores collected from the above optimum growth conditions siloxane-mediated method was used. The lyophilized spores collected by siloxane-mediated method adjusted to 1×10^7 CFU/mL and subjected to spore germination test, OD values at OD_{540} were measured for every 6 h and the corresponding spore samples were photographed simultaneously by SEM to observe the process of spore germination. The results showed that from 6 h there is an increase in the OD values (Fig. 4A) and the germination tube of the spore has been increased (Fig. 4B). Further to confirm the viability of the spores, the spore suspension after 24 h of incubation 50 μL has been inoculated on to the PDA plate and subjected for incubation at 28 °C and the growth was observed for 3 and 12 days (Fig. 4C).

LC-MS analysis and metabolite variations among three stages of *T. sanguinea* ZHSJ

The morphological stages of *T. sanguinea* ZHSJ such as SP, MY and MU were analyzed for the metabolite variations by conducting multivariate analysis. The compounds in methanol extract were analyzed by LC-MS and the data preprocessing identified 3429 positive ions and 3286 negative ions (Fig. 5A) in total 6715 metabolites and these metabolites were analyzed by unsupervised statistical analysis PCA represents the variation of the overall metabolic differences between the samples in each group and the magnitude of variation between the samples was analyzed, here, the QC samples were also analyzed. The PCA score plot represents $R^2X(\text{cum}) = 0.671$ and the metabolite variance of spores, mycelium and fruiting body were separated by PC1 represented 67.10% and PC2 represented 24.60% (Fig. 5B). Further, partial least squares discriminant analysis (PLS-DA) which is supervised

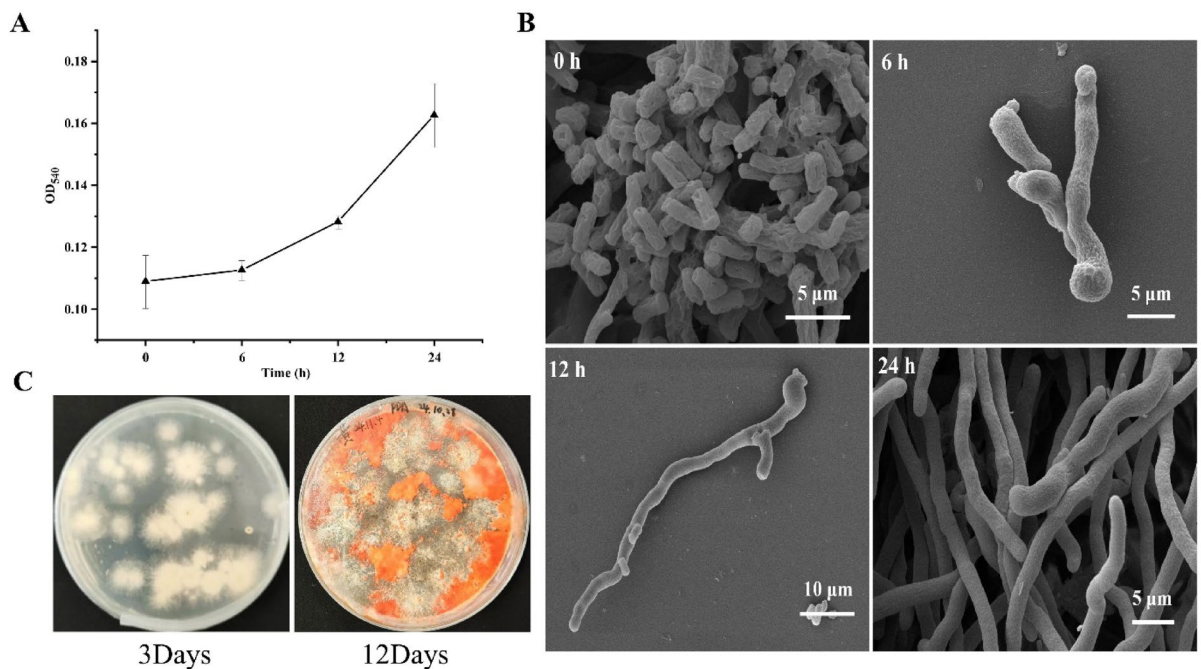


Fig. 4. Spore viability and germination test. (A) The absorbance value of *T. sanguinea* ZHSJ at OD₅₄₀ nm. (B) Observe the spore germination status using SEM. (C) Growth status of spore suspension on PDA plate.

discriminant analysis reveal the metabolites responsible for discrimination in these three morphological stages represents R^2X (cum)=0.923. R^2Y (cum)=0.698 and Q^2 (cum)=0.689 (Fig. 5C). Moreover, the Venn plot represents the common and unique metabolites of SP, MY and MU of *T. sanguinea* ZHSJ (Fig. 5D).

Metabolic variations among three groups

The average ion intensities of three groups represented 13 categories and each category represented significant variation of metabolites (Fig. 6). Among them lipid and lipid like molecules (fatty acids), organic acids (amino acids, peptides and analogues) and organoheterocyclic compounds (nucleic acids) compounds represented highest intensities in all the groups. However, there was a significant metabolite variation among these categories in each group and the variant metabolites of each group were mentioned in (Table S1, S2 and S3).

Differential metabolite cluster and VIP analysis

The differential metabolite analysis refers to the unique and commonly expressed metabolites that are important in metabolic pathways and biological functions between the groups such as SP vs. MU, SP vs. MY and MY vs. MU of *T. sanguinea* ZHSJ (Fig. 7A). Here, in comparison, one on the left represents the experimental group and one on the right represents as the control. Further, differential metabolite analysis also represents the upregulated and downregulated metabolites in comparison of each group, student's t- test with two tailed inspection referred P value < 0.05 and VIP_Pred_OPLS-DA > 1, that represents the metabolites in the classification and discrimination of samples in each group in the model were significantly different. (Fig. 7B). Furthermore, metabolite cluster analysis represents the specific metabolite pattern of expression and their hierarchical clustering among 10 subclusters with top 50 expressed metabolites in each metabolic set i.e. SP vs. MU, SP vs. MY and MY vs. MU (Fig. 7C). Moreover, VIP value of first principal component that influence the expression pattern of biologically significant top 30 metabolites their classification and discrimination in each group were tested and predicted through 7- fold cross validation and significance was represented with $VIP \geq 1$ (Fig. 7D).

KEGG pathway enrichment analysis

The differentially expressed metabolites of group SP vs. MU, SP vs. MY and MY vs. MU possess a specific function. KEGG pathway enrichment analysis represents the functions of the metabolites and their specific pathway. Here, SP vs. MU and SP vs. MY represented the highest number of metabolites, 23 and 31 involved in biosynthesis of co factors, whereas MY vs. MU represented highest number of metabolites involved in diterpenoid biosynthesis (Fig. 8A). Furthermore, the network between these metabolites involved in KEGG pathways has been represented in (Fig. 8B).

Discussion

T. sanguinea possesses several valuable medicinal properties and is an important species used in traditional Chinese medicine²⁹. However, the research on the spores of *T. sanguinea* is very little and its viability analysis was not studied. To our knowledge, this study provides the first insights into the *T. sanguinea* spore identification

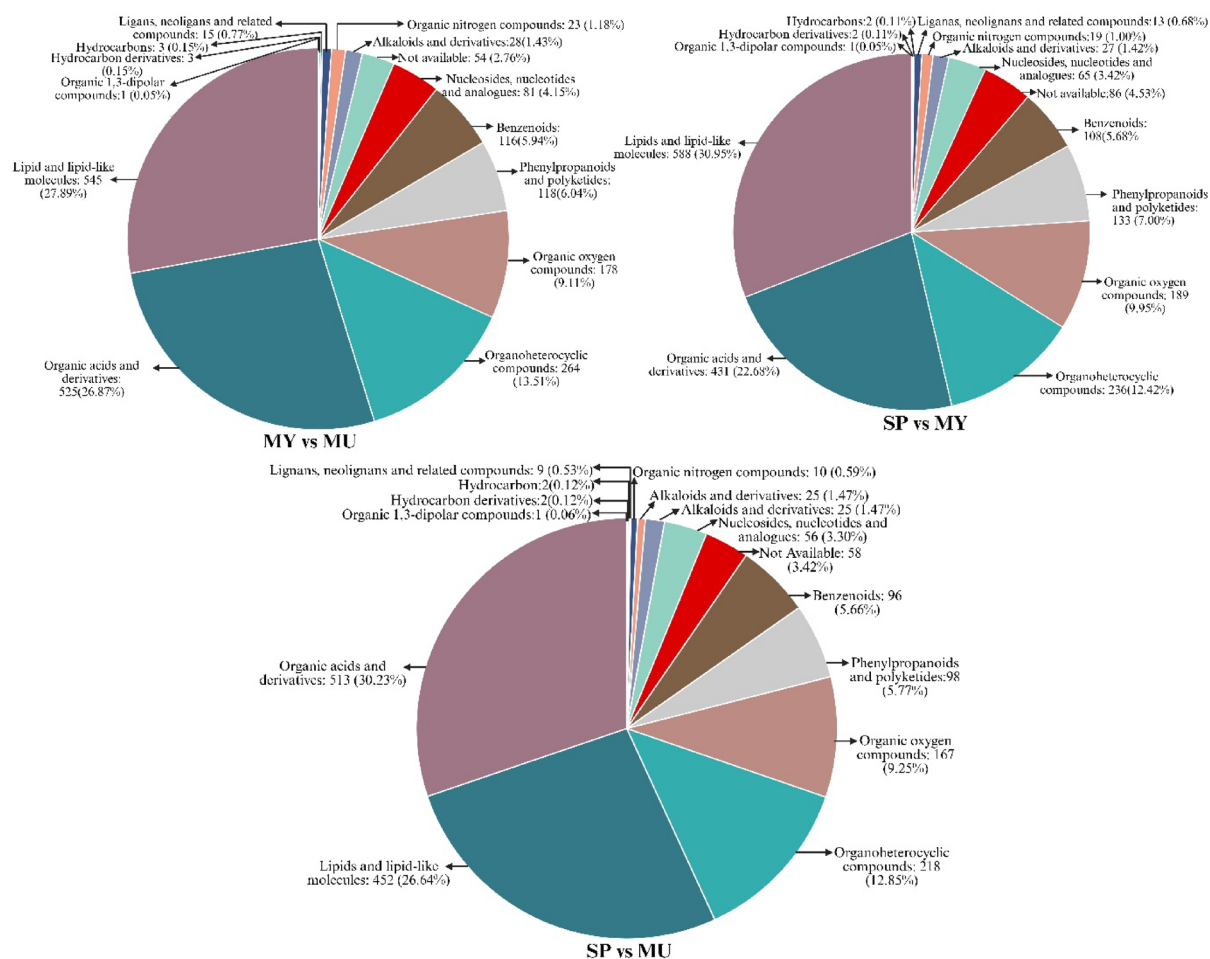


Fig. 6. Metabolic variations. The metabolite variation of the compared groups (MY vs. MU, SP vs. MY and SP vs. MU) has been represented based on the number of metabolites in each category. The different colors represent different categories of metabolites.

at higher culture temperatures because of the low moisture levels, as water evaporates during the growth of fungi³⁴. The data on temperature are consistent with the results of most wood-rotting basidiomycetes which the optimum growth temperature reported is between 20 °C and 30 °C, and no fungi can grow at 40 °C, only five species being able to grow at 35 °C³⁵. In temperate regions, the optimum growth temperature for wood-rot fungi is between 25 °C and 30 °C^{36,37}. The *T. sanguinea* ZHSJ used in this study was collected from Shandong Province, China, which is in the temperate zone. According to relevant experimental reports, fungi prefer glucose over other carbon compounds because glucose can be rapidly metabolized to produce cellular energy³⁸ and the nitrogen source is peptone^{39,40}. Most of the research on the carbon and nitrogen sources of *T. sanguinea* ZHSJ focuses on the production and activity of laccase. For example, *T. versicolor* showed the highest laccase activity after the addition of glycerol, followed by sucrose and glucose⁴¹. When corn steep liquor was used as a nitrogen source to produce laccases by *T. versicolor*, the laccase activity increased by 1.96 times compared to the control medium lacking corn steep liquor⁴². Whereas, for *T. pubescens*, the carbon source that reaches the maximum yield of laccase is maltose, and the nitrogen source is yeast extract, the carbon-to-nitrogen ratio is 5.15:1, which is consistent with the culture results of *T. sanguinea* ZHSJ⁴³.

Trametes species possess several medicinal important compounds that possess several activities such as antimicrobial, antitumor, antioxidant, anti-inflammatory and immunomodulatory effects⁴⁴. Further, our recent research article on whole genome sequencing of *T. sanguinea* ZHSJ of fruiting body represented the annotation and transcriptomic analysis, provided a base study for the current metabolomic study of *T. sanguinea* ZHSJ⁴⁵. However, metabolomics study of co-cultured *Trametes versicolor* and *Ganoderma applanatum* represented varied production of metabolites when compared to individual culturing⁴⁶. Metabolomic differential analysis of interspecific interactions of *Trametes versicolor*, *Pleurotus ostreatus* and *Dichomitus squalens* represented differential metabolites in the interaction zone and metabolites such as carnitine, lipid, ethylene and trehalose were significantly upregulated⁴⁷. Moreover, metabolomics and molecular network analysis of co-cultured *Trametes robiniophila* Murr and *Pleurotus ostreatus* revealed 44 features that were newly produced and significantly high and among them 6 features belong to new family of novel and unusual linear sesterterpenes which possess high antifungal activity⁴⁸. Moreover, metabolomic analysis of brown rot fungi (*Rhodonina placenta* and *Gloeophyllum*

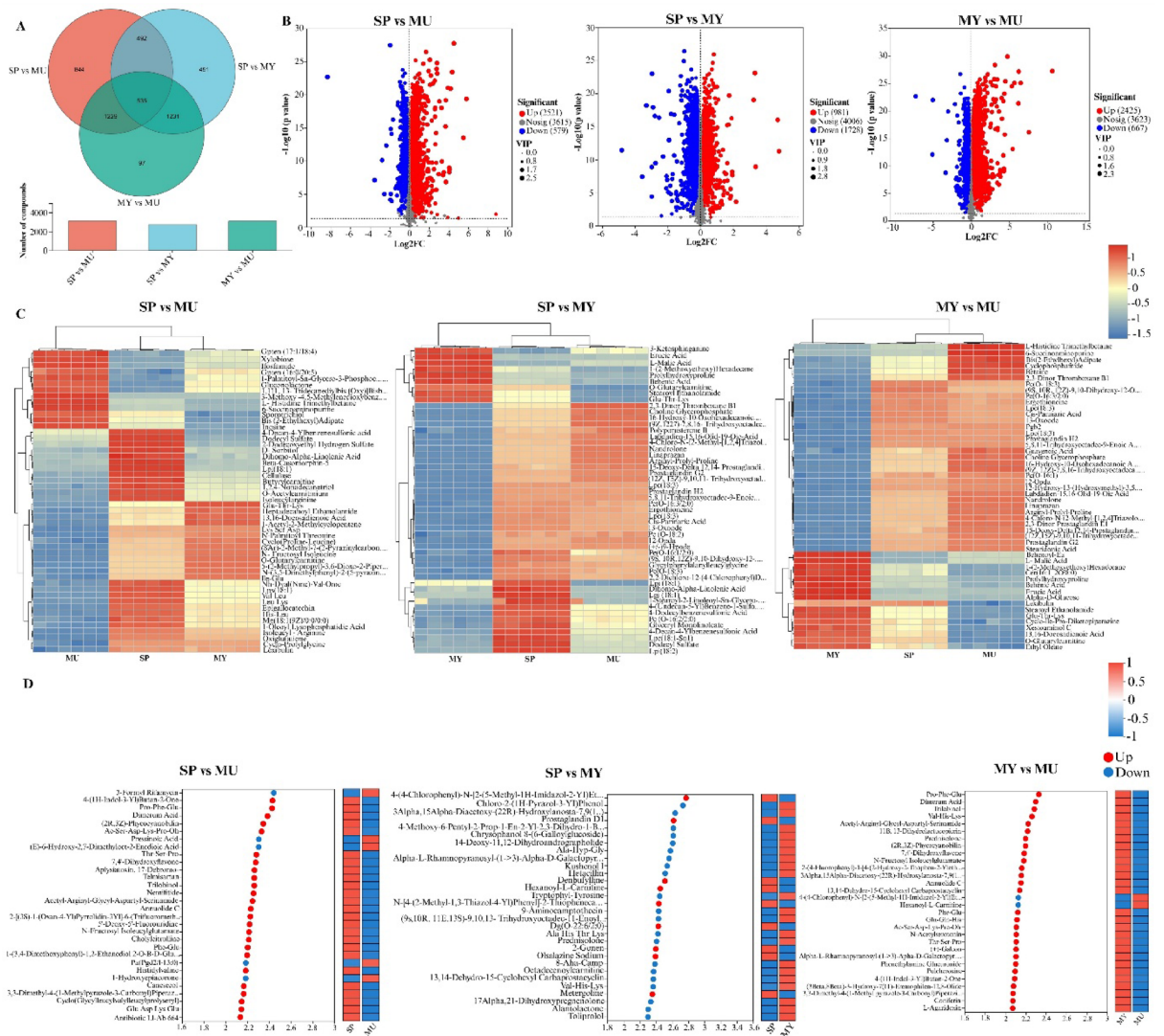


Fig. 7. Differential metabolite analysis. (A) Venn diagram represents the common and differential metabolites of different morphological group comparisons. (B) The volcano plot represents the differential expression of metabolites. Here, Log2FC is the statistical test value of the difference in the expression of metabolites of $-\log_{10}(p \text{ value})$. Each dot represents a specific metabolite, where blue dots represent significant down regulated metabolites, red dot represents significantly upregulated metabolites and gray dots represent non-significant differential metabolites and the size of the dot represents its VIP value. (C) The metabolite hierarchical heat maps represent the differentially expressed metabolites in different groups. Here, each column represents sample and each row represents metabolite and as per the color scale the redder color represents the upregulation of metabolites and bluer represents the downregulation of metabolites and the tree map represents the significant hierarchical relationship between the metabolite's expression. (D) VIP bubble chart represents the expression pattern of each metabolite. Here, Y-axis represents the metabolites and X-axis represents the VIP values. The red color represents the upregulation and blue color represents the down regulation of metabolite in a particular morphological stage.

trabeum) and white rot fungi (*Trametes versicolor* and *Pleurotus ostreatus*) represented significant metabolite variations and white rot fungi has a potential biomarker compound galactitol was identified and white rot fungi were efficient at catabolizing phenolic compounds of wood⁴⁹. However, the current study revealed the metabolic variations of three morphological stages (spores, mycelium and fruiting body) of *T. sanguinea* ZHSJ and achieved spore isolation by utilizing several optimization conditions. Further, studies on these differentially expressed metabolites of spores would lead to identification of potential bioactive compound.

Conclusion

In conclusion, we have achieved isolation of *T. sanguinea* ZHSJ spores by optimizing its growth conditions and then we identified several metabolites that are differentially expressed in spores when compared to mycelium and fruiting body. It was identified that there are 124 metabolites that were peculiar in spore extraction and

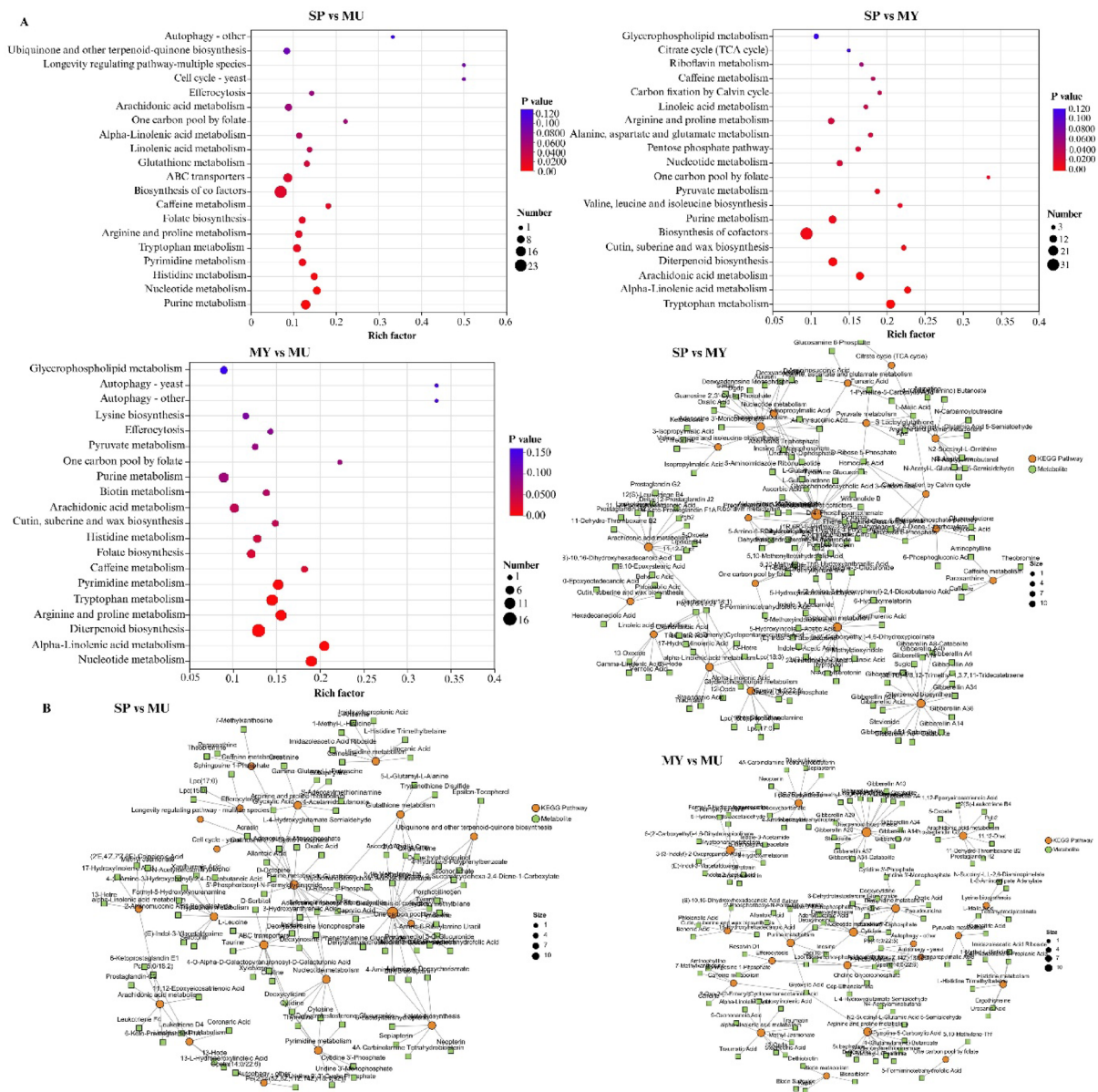


Fig. 8. KEGG enrichment pathway analysis and network of metabolites. (A) KEGG pathway enrichment analysis represents the number of metabolites involved in a group in a particular pathway. Here, the size of the bubble represents the number of metabolites involved and the color represents their significance by p value. (B) KEGG enrichment network diagram represents the pathways and the metabolites involved in specific pathway and their interconnection with other pathways. Here, the green squares represent metabolites and orange circles represent pathways, the more metabolites involved in a pathway the more is the size of the circle^{26–28}.

among them significant number of metabolites belong to organic acids and derivatives, lipids and lipids like molecules and organoheterocyclic compounds. Hence, future studies on biological activities such as antitumor, antioxidant, antimicrobial and anti-inflammatory activities of these metabolites from spores would benefit in the development of novel drugs.

Data availability

T. sanguinea ZHSJ has been stored at China General Microbiological Culture Collection Center with deposit number 40866. Then, its ITS sequence has been deposited in National Center for Biotechnology Information (NCBI) with GenBank accession number PV668984.1 <https://www.ncbi.nlm.nih.gov/nucore/PV668984>.

Received: 11 October 2025; Accepted: 23 February 2026

Published online: 02 March 2026

References

- Lesage-Meessen, L. et al. Phylogeographic relationships in the polypore fungus *Pycnoporus* inferred from molecular data. *FEMS Microbiol. Lett.* **325**, 37–48 (2011).
- Cui, B. et al. Species diversity, taxonomy and phylogeny of *Polyporaceae* (Basidiomycota) in China. *Fungal Diversity* **97**, 137–392 (2019).
- Yan, M. et al. Structural Characterization and Tumor Microvascular Inhibition Activity of Total Polysaccharide from *Trametes sanguinea* Lloyd. *Chem. Biodivers.* **19**, e202100765 (2022).
- Zovckovx, Z. et al. *Mannosidase and Mannanase of Some Wood-rotting Fungi*. (1977).
- Hoshida, H. Isolation of Five Lactase Gene Sequences from the White-Rot Fungus *Trametes sanguinea* by PCR, and Cloning. *Characterization and Expression of the Lactase cDNA in Yeasts*. (2001).
- Sánchez-Corzo, L. et al. Lignocellulosytic enzyme production from wood rot fungi collected in chiapas, mexico, and their growth on lignocellulosic material. *J. Fungi* **7**, (2021).
- Sigoillot, C. et al. Natural and recombinant fungal laccases for paper pulp bleaching. *Appl. Microbiol. Biotechnol.* **64**, 346–352 (2004).
- Brijwani, K., Rigdon, A. & Vadlani, P. V. *Fungal laccases: Production, function, and applications in food processing*. (2010).
- Sakamoto, M. et al. Purification and characterization of a rhamnogalacturonase with protopectinase activity from *Trametes sanguinea*. *Eur. J. Biochem.* **226**, 285–291 (1994).
- Shen, C. et al. Cardioprotective effect of crude polysaccharide fermented by *Trametes sanguinea* Lyoyd on doxorubicin-induced myocardial injury mice. *BMC Pharmacol. Toxicol.* **24**, (2023).
- Lomascolo, A., Uzan-Boukhris, E., Herpoël-Gimbert, I., Sigoillot, J. C., and Lesage-Meessen, L. *Peculiarities of Pycnoporus species for applications in biotechnology*. (2011).
- Zhang, M. et al. Structural characterization of a polysaccharide from *Trametes sanguinea* Lloyd with immune-enhancing activity via activation of TLR4. *Int. J. Biol. Macromol.* **206**, 1026–1038 (2022).
- Zhou, L. et al. Astragalus polysaccharides exerts immunomodulatory effects via TLR4-mediated MyD88-dependent signaling pathway in vitro and in vivo. *Sci. Rep.* <https://doi.org/10.1038/srep44822> (2017).
- Li, J. et al. Purification, structural characterization, and immunomodulatory activity of the polysaccharides from *Ganoderma lucidum*. *Int. J. Biol. Macromol.* **143**, 806–813 (2020).
- Zheng, T. et al. Purification, characterization and immunomodulatory activity of polysaccharides from *Leccinum crocipodium* (Letellier.) Watliag. *Int. J. Biol. Macromol.* **148**, 647–656 (2020).
- He, R., Zhao, Y., Zhao, R. & Sun, P. Antioxidant and antitumor activities in vitro of polysaccharides from *E. sipunculoides*. *Int. J. Biol. Macromol.* **78**, 56–61 (2015).
- Xie, L. et al. Chemical modifications of polysaccharides and their anti-tumor activities. (2020).
- Sun, Y. et al. Biological characteristics, bioactive components and antineoplastic properties of sporoderm-broken spores from wild *Cordyceps cicadae*. *Phytomedicine* **36**, 217–228 (2017).
- Thuy, N. H. L. et al. Pharmacological activities and safety of *Ganoderma lucidum* spores: A systematic review. *Cureus* <https://doi.org/10.7759/cureus.44574> (2023).
- Liu, D., Sun, X., Qi, X. & Liang, C. Sexual spores in mushrooms: bioactive compounds, factors and molecular mechanisms of spore formation. *Springer Sci. Bus. Media Deutschland GmbH* **207**, 38 (2025).
- Jhan, M. H. et al. Enhancing the antioxidant ability of *trametes versicolor* polysaccharopeptides by an enzymatic hydrolysis process. *Molecules* **21**, 1215 (2016).
- Bains, A. & Chawla, P. In vitro bioactivity, antimicrobial and anti-inflammatory efficacy of modified solvent evaporation assisted *Trametes versicolor* extract. *3 Biotech.* **10**, (2020).
- Guo, N. Y. et al. New synthetic approaches for the construction of 2-aminophenoxazinone architectures. *Royal Soc. Chemistry* **28**, (2025).
- Cajka, T. et al. Rapid LC-MS-based metabolomics method to study the Fusarium infection of barley. *J. Sep. Sci.* **37**, 912–919 (2014).
- Zhao, Q., Yang, Z., Zhou, Z., Yang, Y. & Wang, W. Toxicity mechanism of organosilicon adjuvant in combination with S-metolachlor on *Vigna angularis*. *J Hazard. Mater* **480**, (2024).
- Kanehisa, M., Furumichi, M., Sato, Y., Matsuura, Y. & Ishiguro-Watanabe, M. KEGG: Biological systems database as a model of the real world. *Nucleic Acids Res.* **53**, D672–D677 (2025).
- Kanehisa, M. Toward understanding the origin and evolution of cellular organisms. *Protein Sci.* **28**, 1947–1951 (2019).
- Kanehisa, M. & Goto, S. K. E. G. Kyoto Encyclopedia of Genes and Genomes. *Nucleic Acids Res.* **28**, 27–30 (2000).
- Sokovi, M., Glamo Lija, J., Iri, A., Petrovi, J. & Stojkovi, D. Chapter 5 - mushrooms as sources of therapeutic foods. In *Therapeutic Foods* 141–178 (2018).
- Ezike, T. C. et al. Substrate specificity of a new laccase from *Trametes polyzona* WRF03. *Heliyon* **7**, e06080 (2021).
- Mehna, A., Bajpai, P. & Bajpa, P. K. Studies on decolorization of effluent from a small pulp mill utilizing agriresidues with *Trametes versicolor*. *Enzyme Microbial Technol.* **17**, 18–22 (1995).
- Wu, J. et al. Novel salt-tolerant xylanase from a mangrove-isolated fungus *phoma* sp. MF13 and its application in Chinese steamed bread. *ACS Omega* **3**, 3708–3716 (2018).
- Kishimoto, T., Hiyama, A., Toda, H. & Urabe, D. Effect of pH on the dehydrogenative polymerization of monolignols by laccases from *Trametes versicolor* and *Rhus vernicifera*. *ACS Omega* **7**, 9846–9852 (2022).
- Hai, T. T. Incubation temperature affects growth and efficacy of white-rot fungi to improve the nutritive value of rice straw. *Anim. Prod. Sci.* <https://doi.org/10.1071/AN23403> (2024).
- Boddy, L. Effect of temperature and water potential on growth rate of wood-rotting basidiomycetes. *Trans. Br. Mycol. Soc.* **80**, 141–149 (1983).
- Magan, N. Chapter 4 Ecophysiology: Impact of environment on growth, synthesis of compatible solutes and enzyme production. *British Mycological Soc. Symposia Series* 63–78 (2008).
- Ningsih, F., Yanto, D. H. Y., Mangunwardoyo, W., Anita, S. H. & Watanabe, T. Optimization of laccase production from a newly isolated *Trametes* sp. EDN134. IOP Conference Series. *Earth and Environmental Science*. **572**, 012024 (2020).
- Saltarelli, R. et al. A high concentration of glucose inhibits *Tuber borchii* mycelium growth: A biochemical investigation. *Mycol. Res.* **107**, 72–76 (2003).
- Zhang, H., Li, Q., He, P. & Xu, C. Effect of carbon source on properties and antioxidant potential of exopolysaccharides produced by *Trametes robiniophila* (Higher Basidiomycetes). *Int. J. Med. Mushrooms* <https://doi.org/10.1615/IntJMedMushrooms.v17.i2.90> (2015).
- Jin, X. & Wei, S. Efficient short time pretreatment on lignocellulosic waste using an isolated fungus *Trametes* sp. W-4 for the enhancement of biogas production. *Heliyon* <https://doi.org/10.1016/j.heliyon.2023.e14573> (2023).
- Otoni, C., Simões, M. F., Fernandes, S., Santos, C. R. & Lima, N. High laccase expression by *Trametes versicolor* in a simulated textile effluent with different carbon sources and PHs. *Int. J. Environ. Res. Public Health* <https://doi.org/10.3390/ijerph13080778> (2016).
- Wang, F., Hu, J. H., Guo, C. & Liu, C. Z. Enhanced laccase production by *Trametes versicolor* using corn steep liquor as both nitrogen source and inducer. *Bioresour. Technol.* **166**, 602–605 (2014).

43. Velásquez-Quintero, C., Merino-Restrepo, A. & Hormaza-Anaguano, A. Production, extraction, and quantification of laccase obtained from an optimized solid-state fermentation of corncob with white-rot fungi. *J. Clean. Prod.* <https://doi.org/10.1016/j.jclepro.2022.133598> (2022).
44. Lodi, R. S. et al. Current research on the medical importance of *Trametes* species. (2025).
45. Lodi, R. S. et al. Whole genome sequencing and annotations of *Trametes sanguinea* ZHSJ. *Scientific Data* **12**, (2025).
46. Yao, L. et al. Discovery of novel xylosides in co-culture of basidiomycetes *Trametes versicolor* and *Ganoderma applanatum* by integrated metabolomics and bioinformatics. *Sci. Rep.* <https://doi.org/10.1038/srep33237> (2016).
47. Luo, F. et al. Metabolomic differential analysis of interspecific interactions among white rot fungi *Trametes versicolor*, *Dichomitus squaleus* and *Pleurotus ostreatus*. *Sci. Rep.* <https://doi.org/10.1038/s41598-017-05669-3> (2017).
48. Shen, X. T. et al. Unusual and highly bioactive sesterterpenes synthesized by *Pleurotus ostreatus* during coculture with *Trametes robiniophila* Murr. *Appl. Environ. Microbiol.* **85**, e00293-19 (2019).
49. Castaño, J. D. et al. Metabolomics highlights different life history strategies of white and brown rot wood-degrading fungi. *mSphere* <https://doi.org/10.1128/msphere.00545-22> (2022).

Author contributions

Lizeng Peng and Peng Yang collected the wild specimen from the Mengyin Yun Meng scenic area, Linyi city, Shandong Province, China and identified it as *T. sanguinea** and named as *T. sanguinea** ZHSJ. Y.L and Y.S performed the experiments and written the manuscript, X.C and X.Z prepared the figures and L.P, R.S.L, Z.W and C.P reviewed the manuscript.

Funding

This work was jointly supported by the Key R&D Program of Shandong Province (2024TZXD020, 2024TZXD065). The Agricultural Science and Technology Innovation Project (grant number CXGC2025F08) and Research project supported by National Key Laboratory of Natural Product Chemistry at Lanzhou University (grant number 202509).

Declarations

Competing interests

The authors declare no competing interests.

Additional information

Supplementary Information The online version contains supplementary material available at <https://doi.org/10.1038/s41598-026-41835-2>.

Correspondence and requests for materials should be addressed to C.P., L.P., R.S.L. or Z.W.

Reprints and permissions information is available at www.nature.com/reprints.

Publisher's note Springer Nature remains neutral with regard to jurisdictional claims in published maps and institutional affiliations.

Open Access This article is licensed under a Creative Commons Attribution-NonCommercial-NoDerivatives 4.0 International License, which permits any non-commercial use, sharing, distribution and reproduction in any medium or format, as long as you give appropriate credit to the original author(s) and the source, provide a link to the Creative Commons licence, and indicate if you modified the licensed material. You do not have permission under this licence to share adapted material derived from this article or parts of it. The images or other third party material in this article are included in the article's Creative Commons licence, unless indicated otherwise in a credit line to the material. If material is not included in the article's Creative Commons licence and your intended use is not permitted by statutory regulation or exceeds the permitted use, you will need to obtain permission directly from the copyright holder. To view a copy of this licence, visit <http://creativecommons.org/licenses/by-nc-nd/4.0/>.

© The Author(s) 2026